Realizing Human-Robot Cooperative Rope-Spinning with Central Pattern Generator-Based Control Using Visual Information

Kakeru Yamasaki*

The Graduate School of Life Science and Systems Engineering, Kyushu Institute of Technology, Fukuoka, Japan

Koki Iida

The Graduate School of Life Science and Systems Engineering, Kyushu Institute of Technology, Fukuoka, Japan

Patrick Hénaff

LORIA UMR 7503 laboratory, University of Lorraine-INRIA-CNRS, F-54506 Nancy, France ENIB - École Nationale d'Ingénieurs de Brest, Lab-STICC UMR CNRS 6285, Brest, France

Tomohiro Shibata

The Graduate School of Life Science and Systems Engineering, Kyushu Institute of Technology, Fukuoka, Japan

Abstract

Achieving coordinated motion through flexible objects remains a significant challenge in Human-Robot Interaction (HRI). This study investigates a novel application of Central Pattern Generator (CPG) control, previously used in handshake robots, to a rope-spinning task involving human-robot cooperation. A real-time motion feedback system was developed using Azure Kinect, enabling a robot to synchronize its movements with human input by dynamically adjusting CPG outputs. We evaluated the system's performance by varying rope lengths (250– 400 cm) and analyzing spatial trajectories and Euclidean distances between the human and robot end-effectors. Results showed that while high coordination was achieved under shorter rope conditions, longer ropes introduced increased slack and tension variability, which reduced the robot's tracking stability. Frequency analysis also revealed weaker synchronization on the robot side, particularly in the vertical (Z) direction. These findings indicate that vision-based feedback alone is insufficient for robust adaptation to the dynamic characteristics of flexible objects. The vision-based method demonstrated lower amplitude fidelity and synchronization precision than our previous force-feedback approach. Future work will focus on integrating multimodal feedback, combining visual and force sensing, to improve coordination and robustness in flexible-object-mediated HRI.

Keywords: Human-Robot Interaction, Central Pattern Generator (CPG), Rope-Spinning, Flexible Object Manipulation

© 2012, IJCVSP, CNSER. All Rights Reserved



ISSN: 2186-1390 (Online) http://cennser.org/IJCVSP

Article History:
Received: 10/4/2025
Revised: 16/7/2025
Accepted: 1/11/2025
Published Online: 23/11/2025

1. INTRODUCTION

In recent years, as robot technologies continue to advance toward real-world deployment, the demand for robots

*Corresponding author

Email address: yamasaki586868@gmail.com (Kakeru Yamasaki)

that can collaborate with humans has been increasing. Among such efforts, research on Human Robot Interaction (HRI), in which robots adaptively change their behavior in response to human movements, has gained considerable attention in academic and industrial fields.

In HRI, accommodating individual differences, capturing movement and motor characteristics variations among

users, and adapting robot behavior have become a critical challenge. This perspective is particularly emphasized in assistive robotics, where user-specific factors such as physical characteristics and motion rhythms must be considered. In our prior work, we have also investigated control strategies for individual adaptation, particularly in the context of dressing assistance robots [1, 2, 3].

Most prior studies on HRI have focused on physical interaction through rigid bodies, targeting tasks such as handshaking or object handovers [4, 5, 6, 7, 8]. In contrast, HRI involving flexible objects such as ropes or cloth presents additional difficulties due to nonlinear and timevarying physical properties like tension fluctuation and slack. In particular, the realization of synchronized rhythmic movement through flexible objects is an area that has not yet been sufficiently researched.

This study focuses on rope-spinning as a representative HRI task mediated by a flexible object, in which a human and a robot hold opposite ends of a rope and perform coordinated, periodic motion. To enable the robot to adapt to the human's motion in real time, we introduce a biologically inspired Central Pattern Generator (CPG) control strategy, which generates rhythmic motion without relying on explicit external models. CPGs have been widely applied in HRI tasks such as locomotion and handshaking [9], but their application to interaction through flexible objects is still limited.

Inspired by previous work on a handshaking robot, we have studied rope-spinning robots that employ CPG control using force sensors as input [10]. However, other sensory modalities have not yet been explored, and among them, vision plays a particularly important role in sensing human behavior. Therefore, in this study, we propose a method in which the human hand position, obtained using a visual sensor, is fed into the CPG to realize real-time, coordinated rope-spinning motion. We also evaluate how external conditions, such as rope length, affect coordination, and compare the results with force-based feedback to investigate the potential and limitations of CPG control in flexible-object-mediated HRI.

2. RELATED WORKS

As part of our research on cooperative motion between humans and robots through physical contact, we developed a handshake robot [8, 11]. Two major control approaches have been explored for handshake robots: one based on harmonic oscillators derived from physical models, and the other inspired by biological systems, namely CPG control. Harmonic oscillator systems utilize models such as spring-damper dynamics to reproduce periodic motion, but they often require tuning of numerous parameters, making the control design complex [12, 13]. In contrast, CPG control employs nonlinear oscillator networks inspired by neural circuits found in the spinal cord of biological organisms. It is notable for its ability to synchronize with human motion rhythms adaptively [5].

Among these, the Rowat-Selverston model is particularly advantageous, as it can adapt its frequency to the rhythm of an external input by learning a few parameters, enabling flexible synchronization tailored to individuals [14]. The Rowat-Selverston model extends the Van der Pol relaxation oscillator to simulate neuronal behavior and generate adaptive rhythmic signals. Its simplicity and adaptability—requiring only two parameters to switch between discrete and continuous outputs—make it well suited for human-in-the-loop control applications. In prior studies, it has been applied effectively to handshake robots [5, 7]. Jouaiti et al. [15] further demonstrated that the Rowat-Selverston CPG exhibits superior adaptability to human motion compared to other CPG models used in HRI. These characteristics make it a strong candidate for extending rhythmic synchronization to more complex scenarios, such as interaction through flexible objects.

While prior HRI research has predominantly focused on physical contact and synchronization through rigid objects, studies involving flexible objects remain limited. In particular, research addressing the nonlinear physical characteristics of objects such as ropes is scarce. In this study, we extend the CPG control framework previously applied to handshake robots to rope spinning. This application allows us to explore control challenges distinct from those in conventional rigid object-based HRI. The proposed approach is characterized by its ability to adapt to human motion rhythms while accounting for rope tension and slack variations. Notably, it enables human-robot coordination while tolerating the inherent slack and dynamically changing tension of flexible objects, thus representing a novel form of HRI.

3. METHOD

In this study, we aim to realize coordinated rope spinning motions between a human and a robot using the Rowat-Selverston CPG model. An overview of the proposed system is shown in Figure. 1. To adapt the robot's motion to the human's movement, we employ an RGB-D camera, Azure Kinect, which captures human motion in real time. This motion data is input to the CPG controller, enabling dynamically adaptive rope-spinning behavior. Specifically, the skeletal motion data of the human swinging the rope is acquired using Azure Kinect. Based on this input, the CPG generates robot motion. According to the CPG's output, the robot moves in a two-dimensional plane, which learns to synchronize with the human's motion. We also investigate how the coordination behavior of the robot changes with variations in rope length and how such changes affect the cooperative motion.

The Rowat-Selverston CPG model comprises two mutually connected Rowat-Selverston neurons, which can generate periodic signals under specific conditions. These neurons function as adaptive oscillators, producing rhythmically modulated signals in response to external input. The



Figure 1: Overview of the experimental setup used for human-robot cooperative rope-spinning. The human and robot each hold one end of a rope while facing each other. The human motion is captured using Azure Kinect, and the extracted skeletal data are fed into a CPG controller to generate synchronized robot motion in real time.

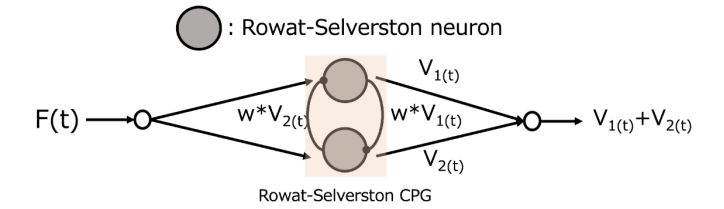


Figure 2: Schematic diagram of the Rowat-Selverston CPG model used in this study. Two mutually inhibitory neurons form a nonlinear oscillator network that produces stable rhythmic outputs. The model adapts its frequency to external inputs, allowing synchronization with human motion.

Rowat-Selverston CPG schematic diagram is presented in Figure. 2. The two neurons are connected via mutual inhibitory coupling, and a stable rhythmic pattern emerges through their interaction.

3.1. Rowat-Selverston CPG

The Rowat-Selverston model extends the Van der Pol relaxation oscillator to simulate rhythmic neuron behaviors, and has been applied to Human-Robot Interaction (HRI) scenarios such as handshake robots [16, 5, 7].

The basic dynamics of each Rowat-Selverston neuron are described by the following equations:

$$\tau_m \dot{V} + V - A_f \tanh\left(\frac{\sigma_f}{A_f}V\right) + q = 0$$
(1)

$$\tau_s \dot{q} = -q + \sigma_s V \tag{2}$$

The variables and parameters used in these equations are summarized below:

- V: membrane potential of the neuron, representing its fast dynamic state.
- q: slow adaptive current that gradually influences the membrane potential.
- τ_m : time constant governing the rate of change of the membrane potential V.
- τ_s : time constant governing the slower dynamics of the adaptive current q.

Table 1: Initial parameters of the Rowat-Selverston neurons.

$ au_m$		A_f				V	1	ϵ
0.35	3.5	0.5	60	1	0.8	0	0	0.1

- σ_s : conductance parameter affecting the slow adaptive current response.
- σ_f : conductance parameter affecting the membrane potential response.
- A_f : scaling factor that sets the saturation amplitude of the membrane potential oscillation.

When an external forcing signal F(t) is applied, the membrane potential dynamics are modified as:

$$\dot{V} = y + \epsilon F \tag{3}$$

where ϵ is the gain for external input, and y represents the intrinsic evolution of V without forcing.

Dynamic Hebbian learning enables the neuron to adapt σ_s to match the external signal F(t), described by:

$$\dot{\sigma}_s = 2\epsilon F \sqrt{\tau_m \tau_s} \sqrt{1 + \sigma_s - \sigma_f} \frac{y}{\sqrt{V^2 + y^2}} \qquad \sigma_f < 1 + \sigma_s$$
(4)

A Central Pattern Generator (CPG) is formed by mutually connecting two such neurons. Each neuron receives input from the external signal F(t) and inhibitory feedback wV(t) from the coupled neuron, enabling adaptive rhythmic synchronization.

The specific parameter values used in this study, determined based on preliminary experiments and previous studies [10], are summarized in Table. 1. In the constructed CPG, two Rowat-Selverston neurons are mutually connected and their membrane potentials are denoted by V_1 and V_2 , respectively. Although V_1 and V_2 are independent variables in principle, we assigned identical initial conditions and identical parameter values to both neurons. Thus, their dynamics evolve symmetrically, and for simplicity, we denote them collectively as V throughout this paper.

4. Experiment

This experiment investigated how variations in rope length affect the robot's ability to maintain synchronized and coordinated motion with a human partner during a rope-spinning task. Rope length was selected as the primary experimental variable, as it influences critical dynamic properties such as slack magnitude, required motion amplitude, and temporal delays in force transmission. These factors are essential for evaluating the robustness and adaptability of the proposed CPG-based control framework under different physical interaction conditions.

Three healthy male participants (age: 23, right-handed) volunteered for the study. Participants were selected to

minimize inter-subject variability in motor performance and to focus on the influence of environmental parameters. Each participant completed trials under four rope length conditions: $250\,\mathrm{cm}$, $300\,\mathrm{cm}$, $350\,\mathrm{cm}$, and $400\,\mathrm{cm}$. These lengths were selected based on preliminary trials to span a range from short, tension-dominated conditions to long, slack-prone conditions, where coordination becomes increasingly difficult.

In each trial, the participant and the robot stood facing each other, holding opposite ends of the rope, and performed continuous rope-spinning movements. To ensure consistent timing across trials and subjects, an auditory cue at 1 Hz was provided, and participants were instructed to match their rope-spinning rhythm to this signal as precisely as possible.

The experiment utilized a Baxter robot, with the rope securely fixed to the end effector of its right arm. The robot's motion was driven by the output of a CPG model, which received input from human motion data. Specifically, the position of the participant's right hand was tracked in real time using an Azure Kinect sensor placed approximately 1.5 m in front of the participant, at shoulder height.

The robot's CPG output controlled two joints in the Y- and Z-directions on a horizontal plane, corresponding to the rope's swing motion. During each trial, the human and robot's motion trajectories were recorded, enabling post hoc analysis of spatial coordination, Euclidean distance fluctuations, and frequency-domain characteristics.

Participants were instructed to maintain a relaxed posture and avoid abrupt movements, focusing on maintaining rhythmic coordination. Each rope length condition was repeated multiple times to ensure consistency, with short breaks between trials to avoid fatigue.

This experimental setup enabled a systematic evaluation of how physical parameters, such as rope length, affect the effectiveness of vision-based CPG control in humanrobot coordination tasks involving flexible objects.

5. Results

As a representative result, Figure. 3 shows the trajectories of the human hand (HH) and the robot end-effector (RH) in the Y-Z plane during the rope-spinning task performed by Subject 1. HH describes a significant circular trajectory, indicating stable periodic motion. In contrast, RH follows a flatter elliptical path with a smaller radius, suggesting insufficient amplitude. Additionally, occasional abrupt disturbances in the robot's trajectory were observed.

Figure. 4 and Figure. 5 present the time-series changes in the Euclidean distance $d_{yz}(t)$ between the human and robot end-effectors in the Y-Z plane, under rope lengths of 250 cm and 400 cm for Subject 1. Here, the Euclidean distance $d_{yz}(t)$ is defined using the robot end-effector coordinates $(y_r(t), z_r(t))$ and human hand coordinates $(y_h(t), z_h(t))$, as shown in Equation (1):

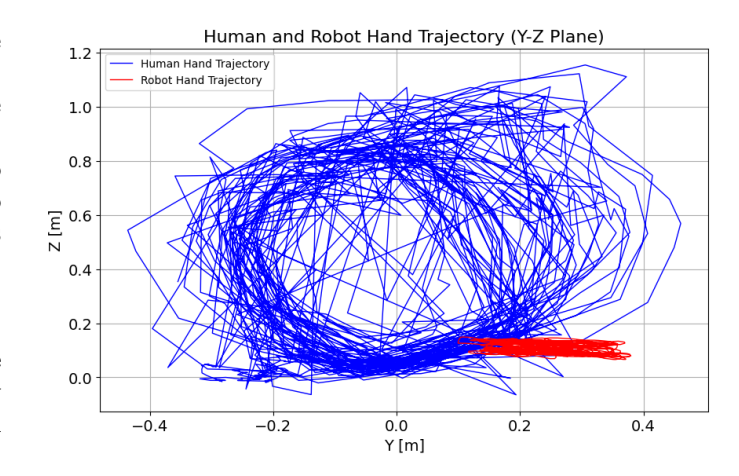


Figure 3: Trajectories of the human hand (HH) and robot endeffector (RH) in the Y-Z plane during a rope-spinning trial by Subject 1. The human trajectory forms a large, smooth circular path, indicating stable periodic motion, while the robot trajectory is flatter and shows irregularities, suggesting limited motion amplitude and occasional desynchronization.

$$d_{uz}(t) = \sqrt{(y_r(t) - y_h(t))^2 + (z_r(t) - z_h(t))^2}$$
 (5)

As Equation (1) defines, the end-effector distance is computed based on the positional difference between the human and robot at each time step. In the 250 cm rope condition (Figure. 4), the Euclidean distance fluctuated periodically within a range of approximately 0.4 m to 1.0 m, indicating relatively stable coordination. In contrast, for the 400 cm rope length (Figure. 5), the distance varied more significantly, ranging from about 0.3 m to 1.4 m, with frequent irregularities and poor periodicity.

Figure. 6 shows the distribution of Euclidean distances between the robot and human end-effectors for Subject 1 across rope lengths of $250\,\mathrm{cm}$, $300\,\mathrm{cm}$, $350\,\mathrm{cm}$, and $400\,\mathrm{cm}$. With a rope length of $250\,\mathrm{cm}$, the median distance was relatively small, and the overall distribution was narrow. As the rope length increased to $300\,\mathrm{cm}$ and $350\,\mathrm{cm}$, both the median distance and variability grew. For Subject 1, the distance distribution became widest at $400\,\mathrm{cm}$, with frequent outliers observed.

Figure. 7 presents the distribution of Euclidean distances for all three subjects under each rope length condition. For all participants, shorter rope lengths generally resulted in lower median distances and less variance. Conversely, longer ropes tended to lead to larger medians and broader distributions, although the degree of widening varied depending on the subject.

Regarding individual trends, Subjects 1 and 3 exhibited a clear tendency for coordination to deteriorate as rope length increased, whereas Subject 2 consistently showed larger fluctuations across all rope length conditions compared to the other subjects, suggesting overall lower coordination stability.

These results highlight that although longer ropes generally made synchronization more difficult, inter-subject

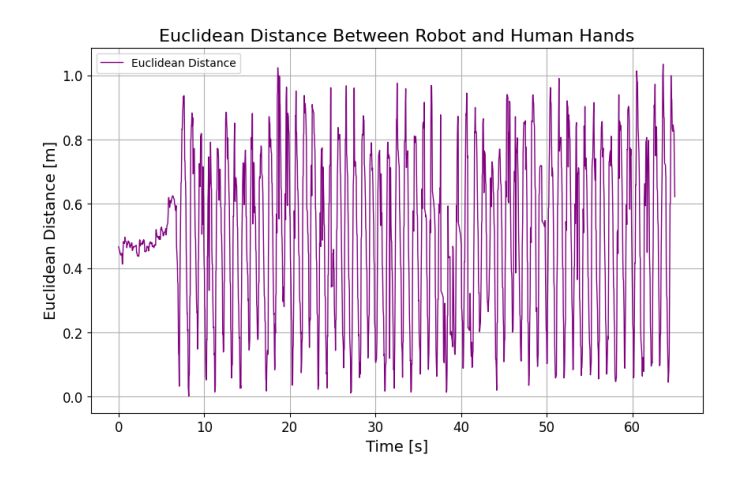


Figure 4: Temporal variation of Euclidean distance between the human hand and the robot end-effector in the Y-Z plane under a rope length of 250 cm. The distance exhibits a stable periodic pattern ranging from approximately 0.4 m to 1.0 m, reflecting consistent coordination between human and robot.

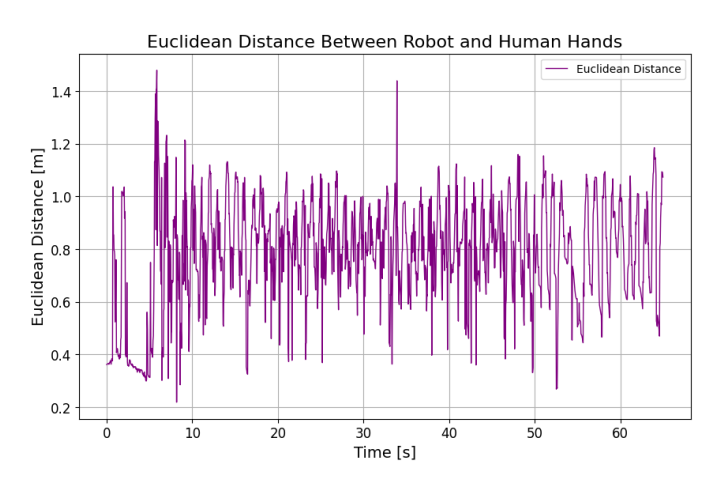


Figure 5: Temporal variation of Euclidean distance between the human hand and the robot end-effector under a rope length of 400 cm. Compared to the 250 cm condition, the distance shows greater fluctuations and irregularities, indicating reduced synchronization and increased difficulty in maintaining coordinated motion.

differences in baseline coordination capability also played a significant role.

The frequency spectra of the Y-coordinates of the human and robot end-effectors for Subject 1 are shown in Figure. 8. A distinct peak near 1 Hz is evident in the HH data, reflecting deliberate rhythmic motion synchronized to the auditory cue. Although a similar peak is also observed in the RH data, its smaller amplitude suggests weaker synchronization.

Figure. 9 shows the frequency spectra of the Z-coordinates. A peak near 1 Hz was also present in the HH data, indicating stable vertical motion. However, similar to the Y-direction, the RH data exhibited lower amplitude, implying insufficient synchronization.

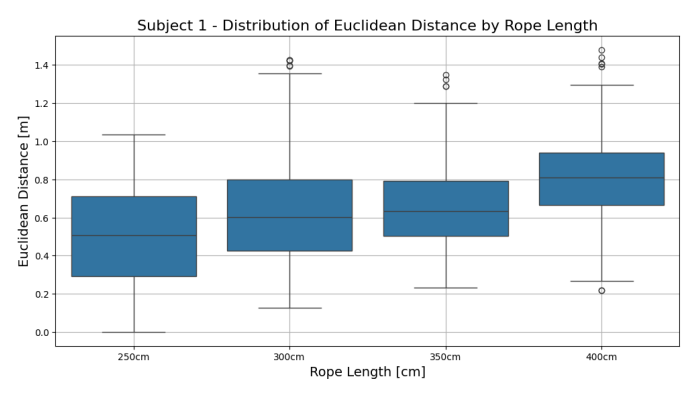


Figure 6: Distribution of Euclidean distances between human and robot end-effectors across four rope length conditions (250 cm, 300 cm, 350 cm, 400 cm) for Subject 1. The results show increasing median distance and variability with longer ropes, with the 400 cm condition exhibiting the widest spread and the most frequent outliers.

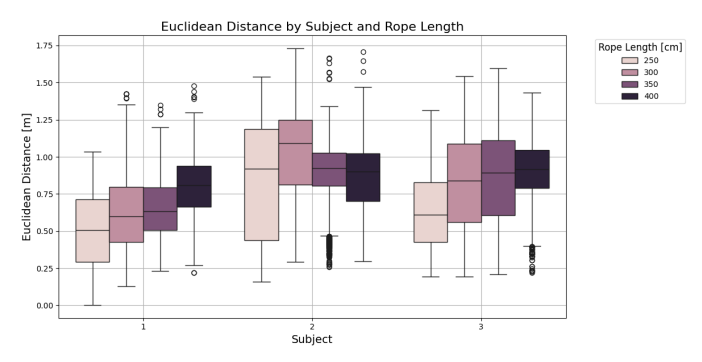
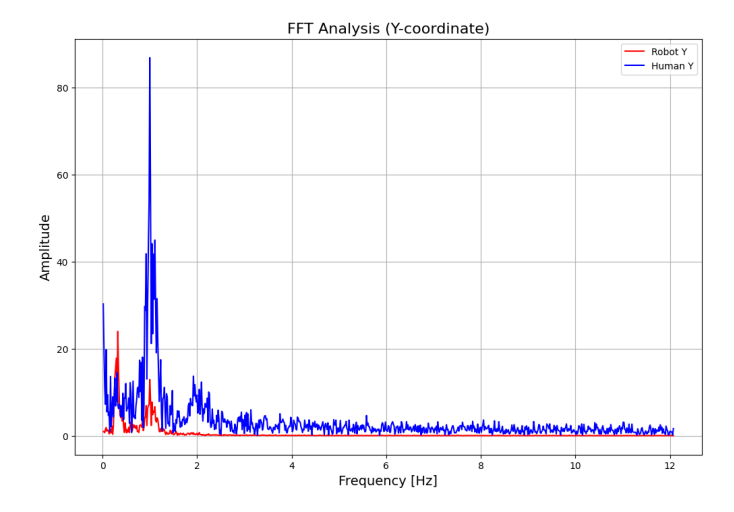


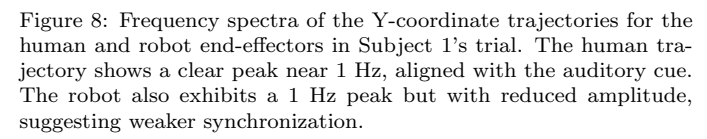
Figure 7: Comparison of Euclidean distance distributions across different rope lengths for all three subjects. Shorter ropes led to lower medians and narrower distributions, while longer ropes caused increased variation and outlier occurrences. Individual differences were observed, with Subject 1 showing the most stable coordination.

6. Discussion

This study analyzed the motion trajectories and distance variations during cooperative rope-spinning between a human and a robot, focusing on how rope length and motion frequency affect coordination. Analysis of the Y and Z coordinates of the end-effector positions revealed that while the human hand maintained a stable circular trajectory synchronized to the 1 Hz auditory cue, the robot's trajectory exhibited significantly smaller amplitudes. This effect was particularly pronounced as the rope length increased, where the robot's amplitude decreased further, and delays or disruptions in its response to the human's motion became more apparent. Sudden irregularities in some trajectory points were also observed.

These findings suggest that longer rope lengths lead to more significant slack and tension variation, making it more difficult for the robot to accurately follow the human's motion. Sudden changes in distance were observed repeatedly, indicating that abrupt tension fluctuations can compromise the stability and precision of cooperative control. Additionally, tracking instability may be partly at-





tributed to occlusions caused by the rope or body parts in the Azure Kinect's skeleton tracking, leading to unstable feedback to the CPG and degraded robot tracking performance.

In the inter-subject analysis, individual differences were observed in the distribution of Euclidean distances, reflecting distinct characteristics in each subject's rope-spinning behavior. These individual differences also influenced the robot's adaptive performance, highlighting the importance of personalized response mechanisms.

The FFT analysis revealed peaks near 1 Hz in both the Y- and Z-axis directions of the robot end-effector (RH). However, the amplitude in the Z-axis was notably small, indicating instability in synchronization along that axis. This is likely due to the limited torque capability of the robot, which is insufficient to maintain adequate rope motion. In particular, rope slack and gravity are more affected by Z-axis motion, requiring greater torque than the Y-axis. In this study, only a single joint was used for Zaxis motion; thus, future focus will be on exploring control strategies involving multiple degrees of freedom. Furthermore, although the CPG parameters and gain settings used in this study were selected based on preliminary experiments and prior work, it is possible that suboptimal tuning contributed to the observed tracking instability. Future work will systematically investigate the influence of different CPG parameter settings, including output and input gains, on coordination stability. Combined with improvements in actuation and sensing, we aim to enhance the robustness of cooperative motion through flexible objects.

In our previous study [10], real-time adaptive control was achieved by feeding back direct tension measurements at the robot's end-effector to the CPG. This force-based approach allowed immediate detection of tension fluctuations and human hand movement, enabling tightly syn-

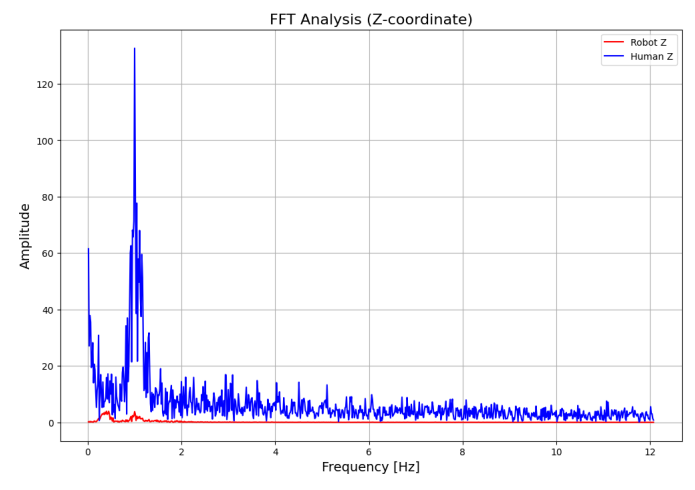


Figure 9: Frequency spectra of the Z-coordinate trajectories for the human and robot end-effectors. Similar to the Y-axis, a peak at 1 Hz is observed in the human motion, while the robot's spectrum shows lower amplitude and irregular frequency components, particularly in the Z-direction where gravity and slack effects are more pronounced.

chronized rhythms between human and robot, and promoting high levels of coordination through physical interaction.

In contrast, this study used 3D positional data estimated by Azure Kinect, feeding the human hand position into the CPG. This visual-feedback-based approach relies on remote sensing, which lacks direct tension information and does not facilitate natural, physically grounded motion guidance. Moreover, Kinect-based sensing is susceptible to occlusion from the rope or body, leading to occasional tracking errors or noise spikes in the coordinates, which can compromise CPG stability.

In both force-based and vision-based input cases, increased rope length exacerbated slack and tension variations, reducing the fidelity of motion transmission from human to robot. This resulted in growing discrepancies in motion rhythms, particularly under long rope conditions, where the robot showed delayed response and more significant fluctuations in Euclidean distance. These results suggest that vision-only feedback is insufficient for rapid adaptation to the rope's physical properties and tension changes.

In conclusion, although this study implemented CPG control with visual feedback, the synchronization accuracy and amplitude reproduction were inferior to those of the force-feedback approach in our prior work. Integrating force/tension information with visual feedback may be a promising direction to achieve more stable trajectories and higher coordination. Future work should improve visual sensing accuracy and realize multimodal control strategies that incorporate visual and haptic modalities.

7. Conclusion

In this study, we extended CPG control, previously used in handshake robots, to human-robot interaction (HRI)

through a flexible object, namely rope-spinning. We developed a system in which a human and a robot cooperatively perform rope-spinning, and investigated the effects of rope length and motion rhythm on coordination. Using the Azure Kinect visual sensor, the human hand position was measured in real time and fed back into the CPG controller, enabling the robot to generate motion adapted to the human's rhythmic movement.

Experimental results showed that when the rope length was short, the robot and human maintained high coordination, and the Euclidean distance between their endeffectors fluctuated periodically in a stable manner. However, as the rope length increased, greater slack and tension variations led to reduced tracking performance in the robot, along with larger fluctuations and abrupt changes in Euclidean distance. Frequency analysis of the Y and Z coordinates revealed that while the human motion exhibited a clear peak near 1 Hz, corresponding to the auditory cue, the robot's peak was smaller in amplitude, particularly in the Z-direction, where spectral irregularities were also observed.

These results indicate remaining challenges in the robot's adaptability to rope length and tension variations. Compared to our previous study, where force-based feedback through direct tension sensing enabled high synchronization and tracking accuracy, the current vision-based approach was less effective in capturing the rope's physical characteristics, leading to decreased amplitude and synchronization accuracy. In particular, hand position sensing with Azure Kinect was vulnerable to occlusion by the rope or body parts, which often caused tracking errors or noise, compromising the stability and precision of the CPG control.

For future work, we plan to introduce integrated feed-back control that combines visual information with tension and force data at the robot's end-effector. This multi-modal approach is expected to enhance adaptive cooperative control by accounting for the rope's physical properties, thereby enabling more stable coordination even under conditions of longer rope lengths and greater tension fluctuations. Ultimately, this approach may offer a promising control framework for HRI involving flexible objects.

ACKNOWLEDGMENT

This research was partially supported by the 2024 joint project between the University of Lorraine and Kyutech.

References

[1] K. Yamasaki, T. Kajiwara, W. Fujita, T. Shibata, Realizing an Assist-As-Needed Robotic Dressing Support System through Analysis of Human Movements and Residual Abilities, in: 2023 32nd IEEE International Conference on Robot and Human Interactive Communication (RO-MAN), 2023, pp. 2409-2414, iSSN: 1944-9437. doi:10.1109/RO-MAN57019.2023.10309329. URL https://ieeexplore.ieee.org/document/10309329

- [2] T. Kajiwara, K. Yamasaki, T. Shibata, Adaptive Dressing Assistance using a Dual Arm Robot for Individual Physique and Kyphosis, in: Proceedings of The 30th Robotics Symposia, Vol. 4C4, Ehime, Japan, 2025.
- [3] K. Yamasaki, T. Shibata, P. Hénaff, Personalized assistance as-needed dressing assistance robot without human modeling using Rowat-Selverston CPG controller, Advanced Robotics 0 (0) 1–16, publisher: Taylor & Francis eprint: https://doi.org/10.1080/01691864.2024.2399728. doi:10.1080/01691864.2024.2399728. URL https://doi.org/10.1080/01691864.2024.2399728
- [4] G. Tagne, P. Hénaff, N. Gregori, Measurement and analysis of physical parameters of the handshake between two persons according to simple social contexts, in: 2016 IEEE/RSJ International Conference on Intelligent Robots and Systems (IROS), 2016, pp. 674-679, iSSN: 2153-0866. doi:10.1109/IROS.2016.7759125.
 URL https://ieeexplore.ieee.org/document/7759125
- [5] M. Jouaiti, L. Caron, P. Hénaff, Hebbian Plasticity in CPG Controllers Facilitates Self-Synchronization for Human-Robot Handshaking, Frontiers in Neurorobotics 12. URL https://www.frontiersin.org/articles/10.3389/fnbot.2018.00029
- [6] M. Costanzo, G. De Maria, C. Natale, Handover Control for Human-Robot and Robot-Robot Collaboration, Frontiers in Robotics and AI 8, publisher: Frontiers. doi:10.3389/frobt.2021.672995.
 - URL https://www.frontiersin.org/journals/robotics-and-ai/articles/10.3389/frobt.2021.672995/full
- [7] A. Melnyk, P. Henaff, Bio-inspired plastic controller for a robot arm to shake hand with human, in: 2016 IEEE 36th International Conference on Electronics and Nanotechnology (ELNANO), 2016, pp. 163–168. doi:10.1109/ELNANO.2016.7493040.
- [8] K. Yamasaki, T. Shibata, P. Hénaff, Individual adaptation and social attributes ${\rm in}$ handshake \mathbf{a} with CPG control. Advanced Robotics (17)(2024)publisher: & 1202-1217. Taylor Francis _eprint: https://doi.org/10.1080/01691864.2024.2384422. doi:10.1080/01691864.2024.2384422. URL https://doi.org/10.1080/01691864.2024.2384422
- [9] A. J. Ijspeert, Central pattern generators for locomotion control in animals and robots: A review, Neural Networks 21 (4) (2008) 642-653. doi:10.1016/j.neunet.2008.03.014.
 URL https://www.sciencedirect.com/science/article/pii/ S089360800800804
- [10] K. Iida, K. Yamasaki, T. Kajiwara, T. SHIBATA, Developing a Rope-Turning Robot for Complex Human-Robot Interactions: An Application of Central Pattern Generators, in: Proceedings of the 12nd International Conference on Robotics and Automation, 2024.
- [11] K. Yamasaki, T. Shibata, P. Henaff, Social Attributes Vary with Individual Differences in a CPG-Controlled Handshake Robot, 2024
- [12] J. Beaudoin, T. Laliberté, C. Gosselin, Haptic Interface for Handshake Emulation, IEEE Robotics and Automation Letters 4 (4) (2019) 4124-4130, conference Name: IEEE Robotics and Automation Letters. doi:10.1109/LRA.2019.2931221. URL https://ieeexplore.ieee.org/document/8772152
- [13] K. Dai, Y. Liu, M. Okui, R. Nishihama, T. Nakamura, Research of human-robot handshakes under variable stiffness conditions, in: 2019 IEEE 4th International Conference on Advanced Robotics and Mechatronics (ICARM), 2019, pp. 744–749. doi:10.1109/ICARM.2019.8833897.
- URL https://ieeexplore.ieee.org/document/8833897
 [14] E. Amrollah, P. Henaff, On the Role of Sensory Feedbacks in Rowat-Selverston CPG to Improve Robot Legged Locomotion, Frontiers in Neurorobotics 4, publisher: Frontiers. doi:10.3389/fnbot.2010.00113.
 - URL https://www.frontiersin.org/articles/10.3389/
 fnbot.2010.00113

- [15] M. Jouaiti, P. Hénaff, Comparative study of forced oscillators for the adaptive generation of rhythmic movements in robot controllers, Biological Cybernetics 113 (5) (2019) 547–560. doi:10.1007/s00422-019-00807-8. URL https://doi.org/10.1007/s00422-019-00807-8
- [16] P. F. Rowat, A. I. Selverston, Modeling the gastric mill central pattern generator of the lobster with a relaxation-oscillator network, Journal of Neurophysiology 70 (3) (1993) 1030–1053. doi:10.1152/jn.1993.70.3.1030.